Article

Anti-Virulence Prospects of Metformin against *Pseudomonas aeruginosa*: A New Dimension to a Multifaceted Drug

Jatin Chadha [1,*], Lavanya Khullar [1], Pallavi Gulati [2], Sanjay Chhibber [1] and Kusum Harjai [1,*]

[1] Department of Microbiology, Panjab University, Chandigarh, India
[2] Department of Microbiology, University of Delhi South Campus, New Delhi, India
* Correspondence: kusumharjai@pu.ac.in (K.H.); chadhajatin0406@gmail.com (J.C.)

Abstract: Metformin (MeT) is an FDA-approved drug with a myriad of health benefits. Besides being used as an anti-diabetic drug, MeT is also effective against various cancers, liver-, cardiovascular-, and renal diseases. It has also been proven to demonstrate anti-ageing and neuroprotective effects. This study was undertaken to examine its unique potential as an anti-virulence drug against an opportunistic bacterial pathogen, *Pseudomonas aeruginosa*. Due to the menace of multidrug resistance in pathogenic microorganisms, many novel or repurposed drugs with anti-virulence prospects are emerging as next-generation therapies with the aim to overshadow the application of existing antimicrobial regimens. The quorum sensing (QS) mechanisms of *P. aeruginosa* are an attractive drug target for attenuating bacterial virulence. In this context, the anti-QS potential of MeT was scrutinized using biosensor assays. MeT was comprehensively evaluated for its effects on different motility phenotypes, virulence factor production (phenotypic and genotypic expression) along with biofilm development in *P. aeruginosa in vitro*. At sub-lethal concentrations, MeT displayed prolific quorum quenching (QQ) ability and remarkably inhibited AHL biosynthesis in *P. aeruginosa*. Moreover, MeT (1/8 MIC) effectively downregulated the expression levels of various QS- and virulence genes in *P. aeruginosa*, which coincided with a notable reduction in the levels of alginate, hemolysin, pyocyanin, pyochelin, elastase, and protease production. *In silico* analysis through molecular docking also predicted strong associations between the QS receptors of *P. aeruginosa* and MeT. MeT also compromised the motility phenotypes and successfully abrogated biofilm formation by inhibiting EPS production in *P. aeruginosa*. Hence, the QQ, anti-virulence, and anti-fouling potential of MeT was elucidated for the first time against *P. aeruginosa*.

Keywords: Metformin; Quorum sensing; Quorum quenching; Pseudomonas aeruginosa; Virulence; Drug repurposing; Anti-virulence therapy; Biofilm inhibition

1. Introduction

The imprudent usage of antimicrobial drugs to treat infectious diseases has given rise to drug-resistance in microorganisms, which has been a serious matter of concern for the global community [1]. With antibiotic resistance outpacing the development of newer antibiotics, this scenario has been snowballing at an unprecedented pace [2,3]. Moreover, pharmaceutical companies have lowered their investments towards formulating novel antimicrobials since the entire process of drug development is excruciatingly expensive and laborious [4]. Hence, there is an urgent demand to formulate novel therapies by either developing new-age antibiotics or through repurposing of existing drugs against drug-resistant infections. In this direction, anti-virulence strategies have emerged as a promising alterative to existing antimicrobial therapies [5]. These attenuate bacterial virulence by abrogating virulence pathways or interfering with the intercellular mechanisms involved in the regulation of virulence genes, such as quorum sensing (QS) [6]. Recent literature has also documented the inhibition of QS pathways as a highly valuable tool to combat bacterial pathogens by directly disarming their intrinsic virulence [5]. Interestingly, unlike conventional antibiotics that mediate bacterial killing, anti-virulence strategies disarm only bacterial virulence without extending any immediate life-or-death scenario over the bacteria. Hence, this lowers the risk of inducing selection pressure, thereby reducing the risk of developing antimicrobial resistance.

Among the extremely notorious bacterial pathogens, *Pseudomonas aeruginosa* is an extensively diverse and multidrug resistant pathogen [6]. This Gram-negative bacterium has been recently categorized pathogen by the World Health Organization as a Priority 1 (critical) superbug [7]. It is majorly associated with a plethora of life-threatening infections in immunodeficient individuals, including cystic fibrosis, burn wound infections, catheter-associated urinary tract infections (CAUTI), keratitis, and ventilator-associated pneumonia [6,8]. Formation of resilient biofilms, production of diverse virulence factors, and wide tissue tropism along with drug resistance mechanisms, make *P. aeruginosa* a versatile and highly invasive bacterial pathogen [6]. Interestingly, the virulence artillery of *P. aeruginosa* is

Preprints (www.preprints.org) | NOT PEER-REVIEWED | Posted: 25 April 2023 doi:10.20944/preprints202304.0914.v1

stringently regulated by the functioning of three QS systems, namely the Las, Rhl, and Pqs [9]. These QS systems are intricately linked to one another and synchronize bacterial behavior at community level to regulate the production of virulence factors like host-damaging enzymes, pigments, toxic secondary metabolites, biofilms, and immune-evasion factors [6]. Recent studies with different quorum quenching (QQ) agents have shown that abrogating QS circuits in *P. aeruginosa* silences virulence and biofilm production [10,11]. Hence, targeting the QS circuitry through identification of novel QQ compounds or drug repurposing can pave way for developing highly efficient, robust, and targeted anti-virulence therapies against *P. aeruginosa*.

Metformin (MeT), a biguanide anti-hyperglycemic drug, routinely prescribed for the management of type II diabetes mellitus which is associated with several other pharmacological benefits including neuroprotective, cardioprotective, anti-ageing, and anti-tumor properties (against breast, colorectal, and endometrial cancers), and management of gestational diabetes, polycystic ovary syndrome, liver and renal diseases, and even obesity [12,13]. Due it its good safety profile (consumption) and low cost, MeT was approved for clinical use by the US FDA in 1994 [12]. There are brief reports highlighting the potential of MeT in augmenting the antimicrobial properties of gold-nanoparticles against *K. pneumoniae*, *S. aureus E. coli*, and *P. aeruginosa* [14]. A recent study concluded that MeT exerts an adjuvant antibacterial effect against *S. aureus* and *P. aeruginosa*, when used in combination with ampicillin, chloramphenicol, doxycycline, levofloxacin, and rifampicin *in vitro* [15]. However, due to the lack of scientific data, MeT has not been used clinically against bacterial infections till date. Hence, the present study was aimed at investigating the new role of MeT as a QQ, anti-virulence, and anti-fouling drug against *P. aeruginosa* using comprehensive *in vitro* experimentation. The study also suggests the probable molecular mechanisms behind the QQ prospects of MeT and substantiates the findings with *in silico* analysis using molecular docking.

2. Results and Discussion

2.1. Effect of MeT on the growth profile of P. aeruginosa

Using the microbroth dilution method, the MIC of MeT against *P. aeruginosa* PAO1 and PA14 was experimentally found to be 100 mg/mL (**Figure S1**). On similar lines, a recent investigation by Masadeh and colleagues have elucidated the antimicrobial properties of MeT against *P. aeruginosa* [15]. Interestingly, MeT has also been shown to act as an antimicrobial adjuvant, subsequently lowering the MICs of antibiotics against pathogenic bacteria [15]. Since this study focuses on scrutinizing the anti-virulence prospects of MeT against *P. aeruginosa*, sub-lethal concentrations of the drug which fail to inhibit bacterial growth, but rather disarm bacterial virulence, were determined initially. Hence, the growth profile of *P. aeruginosa* was monitored at different sub-inhibitory concentrations (sub-MICs: 1/2, 1/4, 1/8, and 1/16) to determine drug concentration(s). The growth curves of both *P. aeruginosa* PAO1 and PA14 (drug-free controls) showed a characteristic sigmoidal growth kinetics with distinguishable lag, log, and stationary phases (**Figure 1**). MeT inhibited the growth of *P. aeruginosa* in a dose-dependent manner. At 1/2 and 1/4 sub-MICs, bacterial growth was remarkably inhibited with the A_{600} values reaching saturation at early time points (**Figure 1**). However, the inhibitory effect was reduced at lower sub-MICs of 1/8 and 1/16, which did not significantly hinder the growth profile of *P. aeruginosa*. Moreover, the growth profile of PAO1 (**Figure 1A**) and PA14 (**Figure 1B**) at 1/8 and 1/16 MIC of MeT closely resembled that of the drug-free controls. This dose-dependent effect can be explained as the concentration of MeT gets empirically reduced to an extent that fails to inhibit bacterial growth. Similar trends have been observed with antibiotics including amoxicillin, gentamicin and nalidixic acid [1,2,11]. Consequently, MeT at sub-MICs of 1/8 (12.5 mg/mL) and 1/16 (6.25 mg/mL) was used for subsequent experimentation.

Preprints (www.preprints.org) | NOT PEER-REVIEWED | Posted: 25 April 2023 doi:10.20944/preprints202304.0914.v1

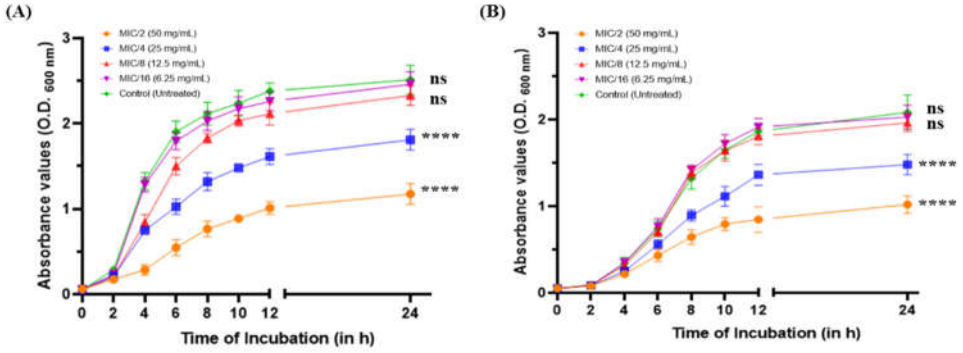

Figure 1. Growth curve of *P. aeruginosa* following treatment with MeT at sub-MICs (A) PAO1 and (B) PA14 (ns: not significant, ****$p \leq 0.0001$).

2.2. MeT disrupts QS by inhibiting AHL production in P. aeruginosa

Recent literature has documented the quintessential role of QS circuits in augmenting the virulence of *P. aeruginosa* [6]. A plethora of antibiotics, phytochemicals, and other repurposed drugs have been reported to harbor anti-QS potential against *P. aeruginosa* at sub-inhibitory concentrations [5]. On similar lines for drug repurposing, the QQ activity of MeT was determined using a recombinant QS biosensor strain, *A. tumefaciens* NTL4, which displays and detects both short- & long-chain AHLs [16]. Interestingly, wells containing MeT at 1/16 MIC (6.25 mg/mL) and 1/8 MIC (12.5 mg/mL) developed a colorless halo (anti-QS zone) around them in a concentration-dependent manner (**Figure 2A**), measuring 13.34 and 18.0 mm in diameter, respectively (**Figure 2B**). The colorless zones obtained with MeT indicated QQ, while the blue coloration (in background) suggested active QS and AHL-dependent production of β-galactosidase, stimulating the enzymatic degradation of X-gal. This biosensor assay provided the first clue hinting towards the anti-QS potential of MeT. Drugs with QQ prospects are known to disrupt QS mechanisms through various mechanisms, including (i) enzymatic breakdown of AHL molecules, (ii) inhibition of AHL production, and (iii) abrogation of signal reception by strongly associating with QS receptor(s) [5]. Since MeT is a pharmacologically active drug and not an enzyme, the latter two scenarios were probed in this study. To investigate the possibilities, a quantitative test was performed to determine the levels of total AHL produced in MeT-treated (test) and -untreated (control) cultures at 1/8 and 1/16 MIC. The production of AHLs in cell-free supernatant of *P. aeruginosa* was analyzed in terms of β-galactosidase activity, as a consequence of AHL-derived induction of *lacZ*, ultimately leading to ONPG hydrolysis. To our interest, treatment with MeT significantly reduced total AHL production in both PAO1 and PA14 in a concentration-dependent manner (**Figure 2C**). At 1/16 MIC, total AHLs were reduced by 22.1% and 20.8% in PAO1 and PA14, respectively. While at 1/8 MIC, AHL production was further lowered by 46.2% and 43.1%, in comparison with the drug-free controls of PAO1 (236.64 MU) and PA14 (313.5 MU), respectively (**Figure 2C**).

Preprints (www.preprints.org) | NOT PEER-REVIEWED | Posted: 25 April 2023 doi:10.20944/preprints202304.0914.v1

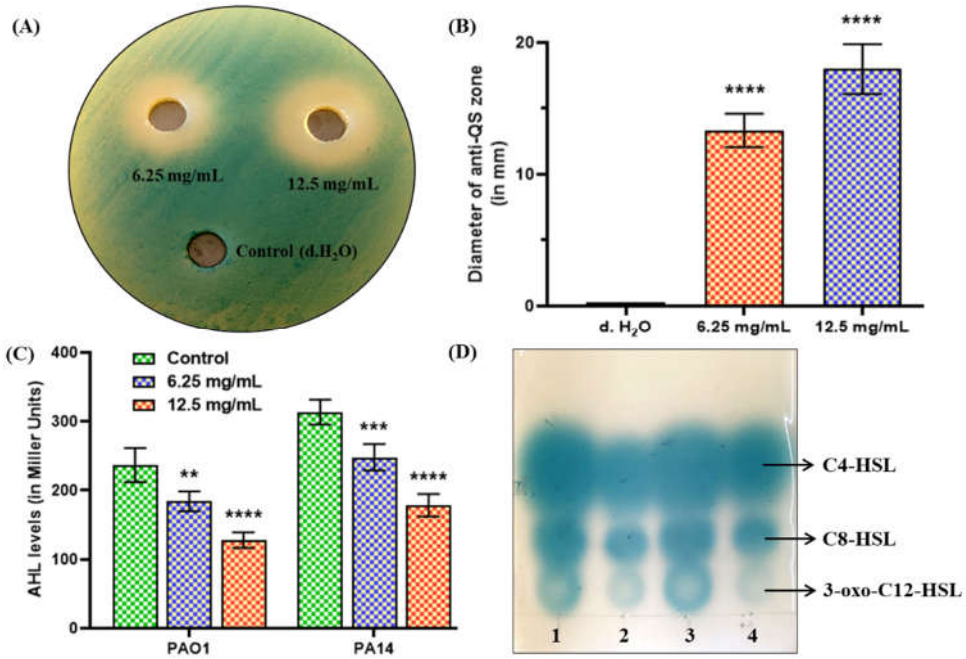

Figure 2. Anti-QS activity of MeT. (A) Qualitative analysis of QQ activity. (B) Graphical representation of anti-QS zones. (C) Quantitative analysis using β-galactosidase assay. (D) TLC agar overlay plate with extract AHLs. Lane 1: *P. aeruginosa* (Control), Lane 2: MeT-treated PAO1, Lane 3: *P. aeruginosa* (Control), Lane 4: MeT-treated PA14 (**$p \leq 0.01$, ***$p \leq 0.001$, ****$p \leq 0.0001$).

These results intrigued us to further investigate and identify the specific AHL molecules that would have been inhibited by MeT at sub-lethal concentrations, a TLC agar overlay method was performed to visualize AHL production in *P. aeruginosa* PAO1 and PA14 following treatment with MeT at 1/8 MIC. This method has been extensively employed and deemed authentic for the visualization of AHL molecules [17]. From the overlaid chromatogram, it was evident that both PAO1 and PA14 strains produce three distinct AHL molecules, i.e., C4-HSL, C8-HSL, and 3-oxo-C12-HSL (**Figure 2D**). Results obtained with the agar overlay method were in accordance with the observations of the β-galactosidase assay, indicating a considerable reduction in AHL production following MeT exposure. The size and color intensity of all blue spots corresponding to different AHLs was notably reduced in both MeT-treated *P. aeruginosa* PAO1 (**Lane 2**) and PA14 (**Lane 4**), as compared to their untreated controls (drug-free) in **Lane 1** and **Lane 3**, respectively (**Figure 2D**). Interestingly, 3-oxo-C12-HSL, which associated with the Las system (keystone QS pathway of *P. aeruginosa*), was inhibited to a higher extent in comparison with other AHLs. Therefore, it could be better correlated that reduction in 3-oxo-C12-HSL levels following MeT exposure interferes with QS in *P. aeruginosa*, which may be consequently held accountable for lowering the levels of C8-HSL and C4-HSL [10]. Similar findings have been reported with other QQ drugs such as ciprofloxacin [18], paeonol [19], and cinnamaldehyde [11], which interfere with AHL biosynthesis in *P. aeruginosa*. Hence, from the present findings, it is concluded that MeT harbors QQ prospects and disrupts the QS by inhibiting AHL production in *P. aeruginosa*.

2.3. MeT associates with QS receptors & possibly inhibits signal transduction in P. aeruginosa

Although MeT was able to effectively curtail QS in *P. aeruginosa* by inhibiting AHL biosynthesis, it was still relevant to probe whether MeT exerts QQ through inhibition of signal transduction. In this direction, computational analysis has proved to be an excellent and robust tool for simulating atomic-level interaction between a ligand and receptor [20]. To virtually investigate this speculation, molecular docking was performed to examine the possible associations between the QS receptors of *P. aeruginosa* and MeT. The binding energies obtained with MeT were compared with that of natural ligands (3-oxo-C12-HSL, C4-HSL, and PQS) and a known QS inhibitor, furanone C-30. The RhlR structure (modelled) was in accordance with the published reports [11,21]. Interestingly, MeT was able to effectively associate with the ligand-binding domains of LasR, RhlR, and PqsR through a myriad of Van der Waal interactions (VdW) (hydrophobic), hydrogen bonds (H-bonds), and π-Cation bonds (electrostatic interaction) (**Figure 3**). It showed

 doi:10.20944/preprints202304.0914.v1

maximum affinity towards LasR (-6.4 kcal/mol), followed by RhlR (-6.0 kcal/mol) and PqsR receptor (-5.8 kcal/mol) (**Table 1**). Multiple amino acid residues on the QS receptors were virtually predicted to interact with MeT. With the LasR receptor, MeT formed VdW interactions with nine amino acid residues, three H-bonds with Tyr56, Thr75, and Thr115, and two π-Cation bonds with Asp73 and Trp88 residues (**Figure 3; Upper Panel**). With the PqsR receptor, MeT formed eleven VdW interactions and three H-bonds with Ala44, Val133, and Ser135 (**Figure 3; Middle Panel**). In association with the RhlR, MeT was shown to form seven VdW interactions, three H-bonds with Ala130, Ser201, and Gln203, and a lone π-Cation bond with Asp150 (**Figure 3; Lower Panel**). Also, several of these amino acid residues (with MeT) also showed common molecular interactions with either furanone C-30 or natural ligand(s) of the specific QS receptor (**Table 1**). Although the binding energies of MeT were significantly lower than the natural ligands of the respective QS receptors, it was numerically comparable to that of furanone C-30 (**Table 1**). The 3D representations of molecular interactions between furanone C-30 and the QS receptors have been depicted in **Figure S2**. In concise, these predictions collectively support the hypothesis that MeT may also abrogate QS circuits by interacting with the QS receptors, consequently abrogating signal transduction. Nonetheless, this speculation warrants further confirmation using molecular dynamic simulations.

Preprints (www.preprints.org) | NOT PEER-REVIEWED | Posted: 25 April 2023 doi:10.20944/preprints202304.0914.v1

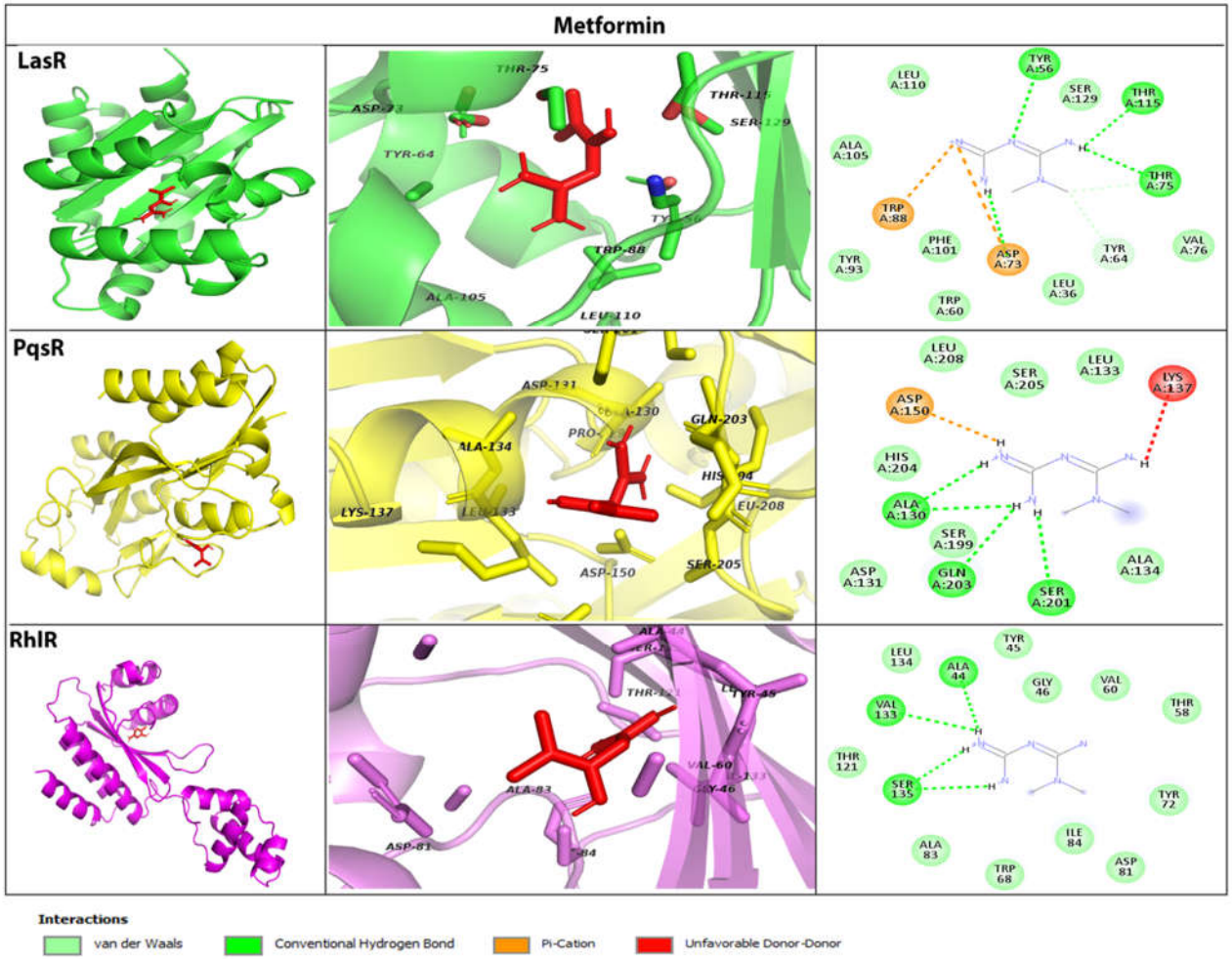

Figure 3. Prediction of molecular interactions between the QS receptors of *P. aeruginosa* and MeT using AutoDock Vina (version 1.2.0).

 doi:10.20944/preprints202304.0914.v1

Table 1. Virtually predicted interactions of LasR, RhlR, and PqsR QS receptors with their natural ligands, metformin, and furanone C-30 in terms of binding energy. **Boldface** amino acid residues of MeT were found to have overlapping interactions with that of either the natural ligand of each QS receptor or furanone C-30.

QS receptors	Ligands	Binding energy (kcal/mol)	Interacting amino acid residues
LasR	3-oxo-C12-HSL	-8.2	Leu36, Gly38, Leu40, Tyr47, Ala50, Ile52, Tyr56, Trp60, Arg61, Tyr64, Ala70, Asp73, Thr75, Val76, Trp88, Tyr93, Phe101, Ala105, Leu110, Leu125, Gly126, Ala127, Ser129
	MeT	-6.4	**Leu36**, **Tyr56**, **Trp60**, **Tyr64**, **Asp73**, **Thr75**, **Val76**, **Trp88**, **Tyr93**, **Phe101**, **Ala105**, **Leu110**, Thr115, **Ser129**
	Furanone C-30	-6.6	Leu36, Tyr47, Ala50, Ile52, Tyr56, Trp60, Arg61, Tyr64, Thr75, Val76, Ala127, Ser129
RhlR	C4-HSL	-7.4	Ala44, Gly46, Trp68, Tyr72, Asp81, Ala83, Ile84, Trp96, Phe101, Leu107, Thr121, Val133, Ser135
	MeT	-6.0	**Ala44**, Tyr45, **Gly46**, Thr58, Val60, **Trp68**, **Tyr72**, **Asp81**, **Ala83**, **Ile84**, **Thr121**, **Val133**, Leu134, **Ser135**
	Furanone C-30	-5.9	Ala44, Val60, Trp68, Tyr72, Asp81, Ala83, Trp96, Leu107, Val133, Ser135
PqsR	PQS	-6.7	Ile149, Gln194, Ser196, Leu197, Leu207, Leu208, Arg209, Pro210, Val211, Phe221, Met224, Ile236, Ile263, Thr265
	MeT	-5.8	His204, **Ala130**, Asp131, Leu133, Ala134, Lys137, Asp150, Ser199, Ser201, Gln203, Ser205, Leu208
	Furanone C-30	-5.7	Ala102, Ser128, Pro129, Ala130, Ile149, Gln194, Leu197, Leu208, Phe221, Ala237, Ile236, Pro238

Preprints (www.preprints.org) | NOT PEER-REVIEWED | Posted: 25 April 2023 doi:10.20944/preprints202304.0914.v1

2.4. MeT suppresses QS and QS-associated virulence genes in P. aeruginosa

The proper functioning of QS mechanisms is critical for the expression of pseudomonal virulence [6]. Henceforth, QS becomes an alluring drug target for attenuating bacterial virulence. Since MeT demonstrated profuse anti-QS activity, it was speculated that this might negatively impact the expression of QS and QS-dependent virulence genes. Hence, qRT-PCR was used to quantify the expression patterns of QS genes, including *lasI*/*lasR*, *rhlI*/*rhlR*, and *pqsA*/*pqsR*, and QS-associated virulence genes encoding LasA protease (*lasA*), LasB elastase (*lasB*), alkaline protease (*aprA*), phospholipase C (*plcH*), and exotoxin A (*toxA*), in PAO1 and PA14, post-exposure with MeT at 1/8 MIC. The relative expression was calculated using Livak's method [22] and GAPDH was used as an internal control. As anticipated, MeT exposure notably downregulated the expression levels of all QS and virulence genes, in both PAO1 and PA14 (**Figure 4**). In PAO1, the *lasI*, *lasR*, *rhlI*, *rhlR*, *pqsA*, and *pqsR* were significantly downregulated by ~ 2.0-, 6.9-, 2.5-, 7.5-, 2.4-, and 4.1-folds, respectively. While in the case of PA14, the downregulation was ~ 3.1-, 6.7-, 2.8-, 7.2-, 2.1-, and 4.8-folds, respectively (**Figure 4**). Moreover, the QS-driven genes, *lasA*, *lasB*, *aprA*, *toxA*, and *plcH*, were remarkably downregulated in PAO1 by nearly 6.9-, 6.7-, 3.4-, 4.1-, and 5.3-folds, respectively. A similar trend was observed with PA14 where the virulence genes were adversely impacted by approximately 6.1-, 6.5-, 3.3-, 3.5-, and 5.9-folds, respectively (**Figure 4**). Collectively, the findings firmly indicate that MeT hinders the QS circuitry, thereby downregulating the expression of QS genes, which in-turn inhibits AHL biosynthesis and consequently suppresses the QS-associated virulence genes in *P. aeruginosa*. These findings are in agreement with previous reports which indicate the suppression of QS and virulence genes in *P. aeruginosa* through inhibition of AHL production following treatment with anti-QS agents like sodium ascorbate [23] and ibuprofen [24]. Hence, MeT can be labelled as a multifaceted pharmacological drug that not only harbors QQ properties, but also suppresses QS and virulence-associated genes in *P. aeruginosa*.

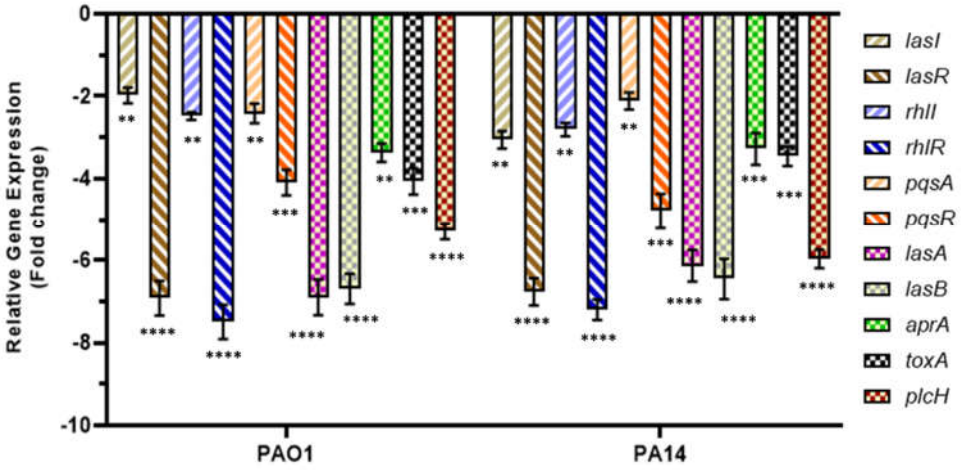

Figure 4. Relative expression of QS- and QS-dependent virulence genes of *P. aeruginosa* PAO1 and PA14 following treatment with MeT at 1/8 MIC. Gene expression has been normalized with GAPDH and depicted relative to the expression of genes in the untreated control (**$p \leq 0.01$, ***$p \leq 0.001$, ****$p \leq 0.0001$).

2.5. MeT displays anti-virulence properties by phenotypically inhibiting the hallmark virulence factors in P. aeruginosa

P. aeruginosa has an extremely diverse virulence artillery which comprises various host-damaging enzymes, beautiful pigments, toxic secondary metabolites, and toxins that enable bacterial colonization, establishment of infection, and disease progression within the host [6]. Their production is stringently regulated by QS circuits, which on activation induce the transcription of virulence genes and operons [9]. Pyocyanin is a blue-coloured secondary metabolite that dysregulates ciliary

 doi:10.20944/preprints202304.0914.v1

function, cellular respiration, calcium homeostasis, promoting pro-inflammatory and pro-oxidant responses, resulting in cell cytotoxicity and ultimately death [6]. Alginate forms an integral part of pseudomonal biofilms as a matrix exopolysaccharide imparting mucoid phenotype, immune evasion, and shielding bacterial cells from the wrath of antibiotics [6]. Hemolysin production stimulates the hydrolysis of membrane phospholipids, causing damage to host tissues and erythrocyte destruction (hemolysis), aiding *P. aeruginosa* in iron acquisition through siderophores [6]. Pyochelin is a low-molecular weight siderophore that scavenges iron from the host microenvironment and also drives inflammatory responses exerting damage to host tissues [6]. In addition, hydrolytic enzymes like LasA protease and LasB elastase induce destruction of host tissues, extracellular matrix proteins, and evasion from host immune system, promoting bacterial invasion and persistent infection [6]. All these constitute the core hallmarks of pseudomonal virulence. Considering the QQ potential and ability of MeT to downregulate the QS and virulence genes, we conjectured that MeT may also function as a potent anti-virulence drug against *P. aeruginosa*. To examine this prospect, standard assays were undertaken to quantitatively estimate the levels of hallmark virulence determinants in MeT-treated and -untreated cell-free supernatants of PAO1 and PA14 at 1/8 and 1/16 MIC. Interestingly, all the test virulence factors were significantly inhibited by MeT in *P. aeruginosa* PAO1 and PA14 at the phenotypic level in a dose-dependent manner (**Figure 5**). At 1/16 MIC, the production of alginate, hemolysin, pyochelin, and pyocyanin in PAO1 was remarkably lowered by nearly 39.1% (5.77 mg/mL), 43.4% (2.13 mg/mL Hb released), 42.9% (A_{510} ~ 0.105), and 44.7% (1.92 µg/mL), respectively (**Figure 5**). In contrast, 1/8 MIC greatly inhibited the production by approximately 66.7% (3.16 mg/mL), 63% (1.39 mg/mL Hb released), 76.6% (A_{510} ~ 0.043), and 71.6% (0.98 µg/mL), respectively in PAO1. A similar trend was observed with PA14 where the test virulence factors were diminished by 50.3% (6.35 mg/mL), 41.4% (2.45 mg/mL Hb released), 35.3% (A_{510} ~ 0.108), and 43.1% (2.78 µg/mL), respectively at 1/16 MIC; while 66.4% (4.29 mg/mL), 64.6% (1.48 mg/mL Hb released), 84.4% (A_{510} ~ 0.026), and 74.9% (1.22 µg/mL) reduction was obtained at 1/8 MIC (**Figure 5**). Interestingly, enzyme activities of bacterial elastase and total cellular protease were also greatly repressed by 31.5% and 28.7% (1/16 MIC), and 57.9% and 69.1% (1/8 MIC), respectively in PAO1. The enzyme activities were significantly lowered by 32.4% and 37.8% (1/16 MIC), while 58.5% and 64.4% reduction was observed in PA14 at 1/8 MIC (**Figure 5**). Additionally, the production of pyocyanin, hemolysin and total bacterial protease was also examined in 10 laboratory-maintained strains of *P. aeruginosa*, following treatment with MeT at sub-lethal concentrations. Intriguingly, all three virulence determinants were remarkably inhibited upon MeT exposure (**Figure S3**). With these conclusive results, our previous findings from the qRT-PCR analysis were successfully translated, thereby asserting that MeT harbors anti-QS and anti-virulence potential against *P. aeruginosa*. Virulence attenuation as a consequence of QS disruption in *P. aeruginosa* has been recently documented in several investigations *in vitro* [25,26]. Similar type of anti-virulence approach has also proven to be successful in protecting *Caenorhabditis elegans* against pseudomonal infections [27,28]. Hence, it is concluded that MeT at sub-inhibitory concentrations is capable of disrupting QS in *P. aeruginosa*, thereby disarming bacterial virulence both at genotypic as well as phenotypic levels.

Preprints (www.preprints.org) | NOT PEER-REVIEWED | Posted: 25 April 2023 doi:10.20944/preprints202304.0914.v1

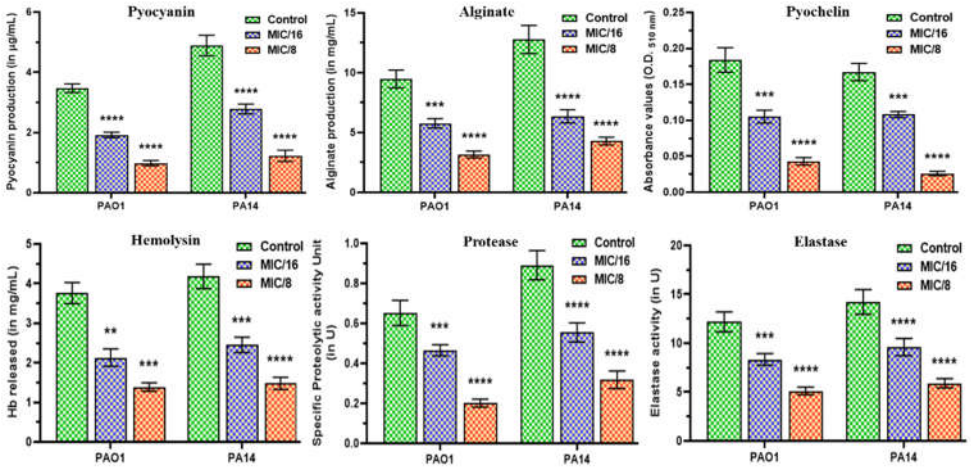

Figure 5. Phenotypic expression of QS-regulated virulence factors (pyocyanin, alginate, pyochelin, hemolysin, protease, and elastase production) in *P. aeruginosa* following treatment with MeT (**$p \leq 0.01$, ***$p \leq 0.001$, ****$p \leq 0.0001$).

2.6. MeT retards the motility phenotypes of P. aeruginosa

Bacterial motility plays an important role in facilitating surface colonization, escaping host defense mechanisms, resisting counter flow, promoting biofilm formation, and enabling bacteria to compete and co-exist in polymicrobial biofilms [6]. Depending on the nutrient availability and physical properties of the colonizing surface, *P. aeruginosa* is capable of transitioning between its motility phenotypes through modulation of type IV pilus or bacterial flagella [29]. Interestingly, these phenotypes of *P. aeruginosa* are greatly influenced by QS, particularly swimming and swarming motility [30,31]. Since MeT displayed anti-QS and anti-virulence properties, we were intrigued to examine its effects on the pseudomonal motility phenotypes. All types of pseudomonal motilities were significantly impeded in the presence of MeT at both the test concentrations (**Figure 6**). In accordance with the previous results, the anti-motility effects of MeT were also found to be dose-dependent, with maximum inhibition observed at 1/8 MIC. The diameters of bacterial growth on different motility media have been documented in **Table 2**. In comparison with the control (untreated), the twitching, swarming, and swimming motility of PAO1 was significantly compromised by nearly 17.6%, 31.2%, and 27.6%, respectively at 1/8 MIC (**Figure 6; Upper Panel**). Similarly, the motility phenotypes of PA14 were also notably inhibited by approximately 43.1%, 45.1%, and 23.7%, respectively (**Figure 6; Lower Panel**). Considering the importance of type IV pilus and flagella and in modulating the motility phenotypes in *P. aeruginosa*, it may be speculated that their impaired functioning results in lowered bacterial motility. Moreover, recent investigations have also confirmed the QQ prospects of phytocompounds like cinnamaldehyde and α-terpineol for impeding pseudomonal motilities [10,11]. In concise, these results further elucidate that MeT at sub-inhibitory concentrations impedes the pseudomonal motility phenotypes, which may ultimately affect bacterial pathogenesis and negatively impact disease progression.

Preprints (www.preprints.org) | NOT PEER-REVIEWED | Posted: 25 April 2023 doi:10.20944/preprints202304.0914.v1

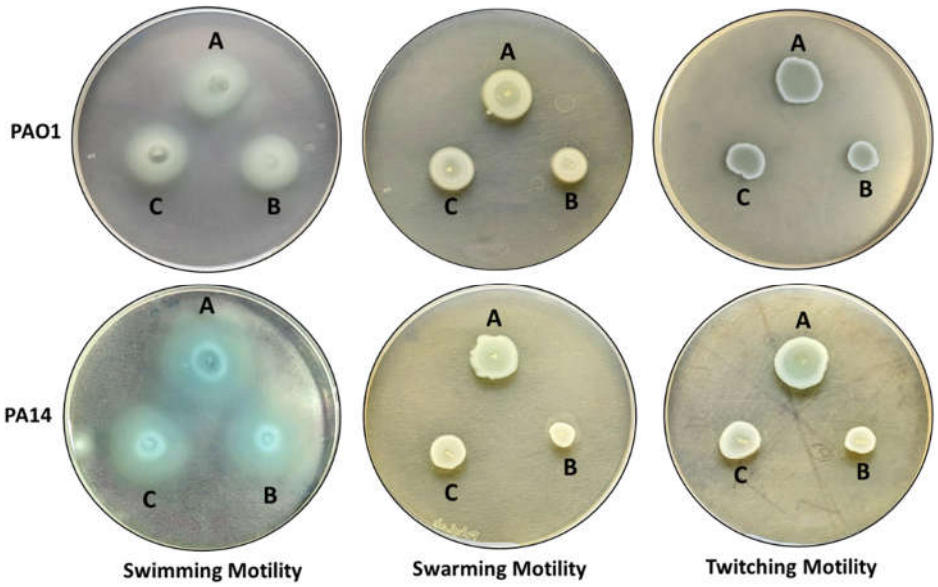

Figure 6. Swimming, swarming, and twitching motility of *P. aeruginosa* PAO1 and PA14 following treatment with MeT at different sub-MICs. (A) Untreated control, (B) MeT at 1/8 MIC, (C) MeT at 1/16 MIC.

Table 2. Diameters of bacterial growth obtained on different motility media following treatment with MeT at sub-lethal concentrations.

Motility Phenotype	Diameter of bacterial growth (in mm) ± Standard Deviation					
	PAO1			PA14		
	Control	1/8 MIC	1/16 MIC	Control	1/8 MIC	1/16 MIC
Swimming	42.34 ± 3.0767	30.67 ± 2.804	35.167 ± 2.639	35.83 ± 0.983	27.34 ± 1.032	30.34 ± 1.861
Swarming	18.167 ± 0.408	12.5 ± 0.547	14.5 ± 0.547	17.0 ± 0.894	9.34 ± 1.211	12.67 ± 0.816
Twitching	19.834 ± 1.169	16.34 ± 0.816	17.5 ± 0.836	18.34 ± 0.816	10.41 ± 0.491	13.167 ± 0.752

2.7. MeT inhibits biofilm development by abrogating EPS production in P. aeruginosa

Biofilm production in *P. aeruginosa* is regarded as the principle virulence hallmark responsible for imparting drug resistance towards penetration of antimicrobial drugs, phagocytosis by immune cells, oxidative stress, and nutrient depletion [32]. Importantly, the QS pathways of *P. aeruginosa* are known to positively impact biofilm formation by aiding the transition of bacterial cells between microcolony formation, biofilm maturation, and persistence [6]. Moreover, pseudomonal biofilms are known to be a serious challenge in clinical setups, especially in patients instilled with invasive medical devices like urinary catheters [8]. Hence, drugs targeting the QS circuitry may also be repurposed as anti-fouling agents against *P. aeruginosa*. With this notion, we performed quantitative biofilm inhibition assays and standard procedures for the quantitative estimation of total biofilm protein and polysaccharide content in PAO1 and PA14 biofilms following MeT treatment. Both the strains of *P. aeruginosa* exhibited strong biofilm-forming capabilities, which gradually escalated following prolonged incubation at 37ºC, attaining a peak on the fourth day (**Figure 7A & B**). PAO1 and PA14 biofilms showed a steady decline on the fifth day, indicating the onset of biofilm maturation and dispersion. Notably, sub-lethal concentrations of MeT could significantly lower biofilm development in a concentration-dependent manner. At 1/16 MIC, MeT was able to reduce the development of pseudomonal biofilms by delaying biofilm maturation (**Figure 7A & B**). On their respective peak day, MeT (1/16 MIC) inhibited biofilms of PAO1 and PA14 by nearly 25.8% and

 doi:10.20944/preprints202304.0914.v1

19.8%, respectively, in comparison with the drug-free controls. Contrarily, supplementing MeT at 1/8 MIC substantially compromised biofilm production throughout the course of experimentation. Neither of the *P. aeruginosa* biofilms attained any maxima, nor did they display any maturation or dispersion (**Figure 7A & B**). Rather PAO1 and PA14 biofilms were impeded by 79.1% and 77.8% on the fifth day, with respect to the control groups. Hence, these findings hinted towards the anti-fouling prospects of MeT.

Additionally, the results from CV-binding assays were further in-sync with the experimental outcomes that estimated the pseudomonal biofilm components. To our interest, treatment with MeT remarkably reduced the total biofilm proteins and exopolysaccharide content in both PAO1 and PA14 biofilms with high level of significance (**Figure 7C & D**). In reference with the untreated controls, maximum inhibition of biofilm components was achieved with MeT at 1/8 MIC, while 1/16 MIC exerted a lower degree of inhibition. At 1/8 MIC, total protein content in PAO1 and PA14 biofilms was reduced by 65.1% and 47.4%, respectively (**Figure 7C**). On the other hand, exopolysaccharide content was lowered by nearly 78.2% and 74.9%, respectively (**Figure 7D**). Experimental procedures were further extended by qualitative detection of changes in eDNA profiles of MeT-treated and -untreated biofilms. As anticipated, a comparable trend was noticed wherein the eDNA release was lowered upon MeT treatment (**Figure 7E**). In both PAO1 and PA14 biofilms, eDNA release was inhibited in a concentration-dependent manner, in comparison with their drug-free counterparts. Hence, this provided strong evidence pointing towards the anti-fouling abilities of MeT against *P. aeruginosa*. To validate these experimental findings, MeT-treated and -untreated pseudomonal biofilms (mature: four-day old) were visualized using FESEM. Both PAO1 and PA14 (control) showed intense biofilm formation, which was characterized by the presence of a dense extrapolymeric layer (EPS) around the bacterial cells (**Figure 8; First Vertical Panel**). Correlating all our previous findings, MeT was able to alter the biofilm architecture and prevent bacterial adhesion, without killing any bacterial cells. A dose-dependent effect was observed against both PAO1 and PA14 biofilms (**Figure 8**). *P. aeruginosa* biofilms were revoked at both 1/16 MIC (**Figure 8; Second Vertical Panel**) and 1/8 MIC (**Figure 8; Third Vertical Panel**). Cell adhesion was also notably lowered at 1/8 MIC, which was visualized by the reduction in cell number per microscopic field. Recent studies have also reported the anti-fouling prospects of other repurposed drugs that possess profound anti-QS activity against *P. aeruginosa*, including paracetamol [26] and ibuprofen [24]. Inhibition of EPS production along with lowered eDNA release and total biofilm protein are also known to augment the anti-virulence potential of phytochemicals *in vitro* [10,11]. In summary, our findings indomitably illustrate the anti-biofilm prospects of MeT by abrogating EPS production and bacterial cell adhesion in *P. aeruginosa*. Hence, based on the *in vitro* findings obtained from this study, it is culminated that MeT may be repurposed against *P. aeruginosa* since it functions as a multifarious drug that harbors QQ potential along with exceptional anti-virulence and anti-fouling capabilities.

Preprints (www.preprints.org) | NOT PEER-REVIEWED | Posted: 25 April 2023 doi:10.20944/preprints202304.0914.v1

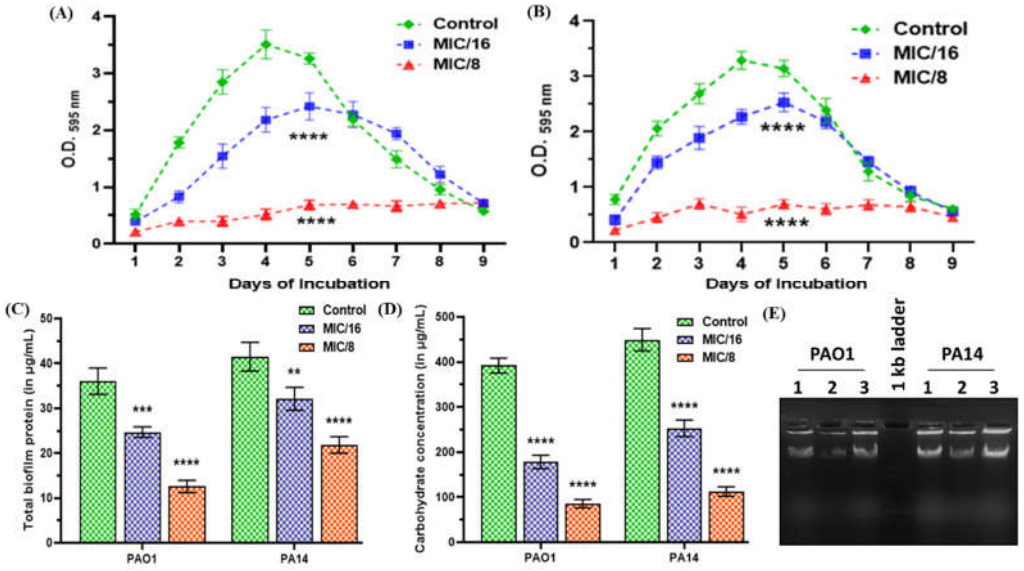

Figure 7. Effects of MeT on biofilm production in *P. aeruginosa*. Quantitative CV-binding assays depicting the biofilm formation pattern of (A) PAO1 and (B) PA14. Comparative estimation of total biofilm (C) protein and (D) polysaccharides. (E) eDNA profiles of pseudomonal biofilms post-MeT treatment (ns: not significant, $^{**}p \leq 0.01$, $^{***}p \leq 0.001$, $^{****}p \leq 0.0001$).

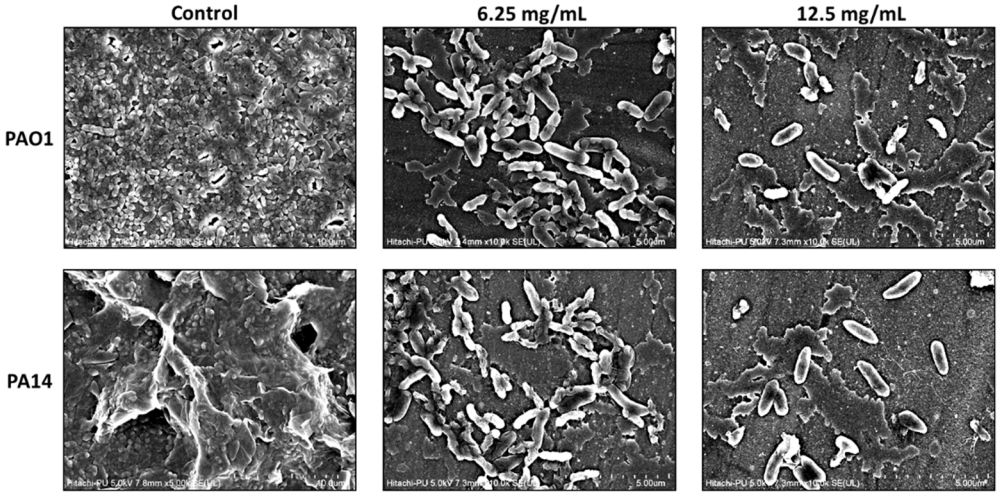

Figure 8. Microscopic visualization of mature *P. aeruginosa* biofilms following treatment with MeT using FESEM.

3. Materials and Methods

3.1. Bacterial strains, culture conditions, and chemicals

The standard *P. aeruginosa* strains, PAO1 and PA14, were acquired from Dr. Barbara H. Iglweski of the Department of Microbiology and Immunology at the University of Rochester (NY, USA) and Dr. Jogender Singh, Department of Biological Sciences, IISER Mohali, India, respectively. *Agrobacterium tumefaciens* NTL4 (pZLR4), an AHL-deficient QS biosensor strain, was obtained from Dr. Jo Handelsman of Wisconsin University (WI, USA). *P. aeruginosa* strains were cultured in Luria Bertani (LB) broth (HiMedia Labs, Mumbai, India) at 37ºC, while *A. tumefaciens* NTL4 was grown in LB broth supplemented with gentamicin (50 µg/mL) at 30ºC. Medical-grade Metformin (MeT) was purchased from Cipla Limited (Mumbai, India) and dissolved in sterile distilled water. For all experimental procedures, drug-free bacterial cultures were used as positive control.

Preprints (www.preprints.org) | NOT PEER-REVIEWED | Posted: 25 April 2023 doi:10.20944/preprints202304.0914.v1

3.2. Determination of minimum inhibitory concentration (MIC)

The MIC of MeT was determined against *P. aeruginosa* PAO1 and PA14 using the microbroth dilution method, following standard protocols [33]. In brief, serial dilutions of MeT were prepared in double-strength MH broth. Bacterial inoculum (1 x 10^8 CFU/mL) was added to the drug dilutions and incubated at 37°C for 24 h. Negative control contained only sterile media, while positive control lacked MeT. After incubation, 0.01% resazurin (Sigma-Aldrich, MO, USA) was dispensed into the wells and the plate was further incubated for 2 h. The MIC was defined as the lowest concentration of MeT that failed to reduce resazurin (blue) to resorufin (pink).

3.3. Growth analysis at sub-MICs

The growth pattern of *P. aeruginosa* PAO1 and PA14 was studied following treatment with MeT at different sub-MICs. LB medium supplemented with MeT at 1/2, 1/4, 1/8, and 1/16 MIC was inoculated (1%) with overnight bacterial cultures and incubated at 37°C with shaking at 180 rpm [2,10]. Positive-growth controls were established with inoculated LB medium without MeT. After 2 h interval, 1 mL aliquots were drawn and the growth pattern was monitored over a 24-h period by recording the changes in absorbance values at 600 nm. Sub-lethal concentrations of MeT that failed to retard bacterial growth were chosen for further experimentation.

3.4. AHL extraction and biosensor assay for determining the QQ potential

AHLs were isolated from *P. aeruginosa* PAO1 using a previously established solvent extraction method [10]. The QQ potential of MeT was then evaluated using a qualitative assay employing *A. tumefaciens* NTL4 biosensor strain [11]. Briefly, LB agar was sequentially spread-plated with 150 µL each of X-gal (8 mg/mL in DMF) and extracted AHLs, followed by uniformly swabbing 200 µL of *A. tumefaciens* NTL4 culture. Using a sterile borer, wells were made into the freshly-seeded plate and 100 µL of MeT (sub-MICs) was dispensed into them. The plate was incubated at 30ºC for 48 h and the diameter of anti-QS zones (with colourless halo) were recorded. Distilled water (sterile) was employed as the solvent control.

3.5. Agar overlay method to assess AHL production

To detect the levels of different AHL molecules in *P. aeruginosa* following MeT treatment, a modified thin-layer chromatography (TLC) agar overlay assay was employed [10]. Briefly, AHL molecules were isolated from MeT-treated and -untreated cultures (200 mL) of *P. aeruginosa* using solvent extraction method. Next, extracted AHLs from different experimental groups were loaded (50 µL) onto a TLC plate (reverse phase). The components were resolved using MeOH/water (60:40 v/v) as the solvent front in a saturated glass chamber. Next, *A. tumefaciens* NTL4 culture and X-Gal were dispensed into molten soft agar (20 mL), which was immediately casted on top of the resolved TLC plate (air dried). The overlaid chromatogram was then incubated at 30ºC for 48 h to enable the development of discrete blue-coloured spots corresponding to different AHL molecules. The intensity of each spot was compared to that of control lane to examine the level of different AHLs produced by *P. aeruginosa* PAO1 and PA14.

3.6. Quantitative estimation of total AHL production using β-galactosidase assay

Total AHL production in experimental (treated) and control (untreated) groups was assessed in terms of β-galactosidase activity [10]. Briefly, extracted AHL mix (10 mL) was dispensed into *A. tumefaciens* NTL4 culture (50 mL) and incubated at 30ºC for 12 h. Bacterial cells were harvested by centrifugation, followed by resuspending the pellet in 10 mL of Z-buffer and recording the absorbance value at 600 nm. Cell lysate (1 mL) was prepared by adding 100 µL chloroform and 0.1% SDS, followed by vigorous mixing. Next, o-nitrophenyl-D-galactopyranoside (400 µL) was added and the enzymatic reaction was allowed to proceed at 30 ºC for 4 h. The reaction was then terminated using Na_2CO_3 (1 M) and the A_{420} value was recorded. β-galactosidase activity was assessed to

Preprints (www.preprints.org) | NOT PEER-REVIEWED | Posted: 25 April 2023 doi:10.20944/preprints202304.0914.v1

quantify total AHL levels using the following formula [10]: β-galactosidase activity (in Miller Units) = A_{420nm} x 1000 / Time (min) x Volume of culture (mL) x A_{600nm}.

3.7. Ligand standardization and molecular docking studies

The Protein Data Bank (PDB) (https://www.rcsb.org/) was used to acquire the spatial coordinates of LasR (PDB: 3IX3) and PqsR (PDB: 4JVC). Since the structure of RhlR is unknown, its protein sequence (UniProtKB ID: P54292) was obtained from the UniProtKB database (http://www.uniprot.org/). Rosetta Comparative Modelling (Rosetta Server) was used to conduct homology modelling [11]. The resulting model was validated *via* MolProbablity, Verify3D, and ERRAT servers based on the stereochemical and geometric parameters analysis. GROMACS software suite (v2020.6) was then employed for energy minimization of the structures using the CharMM36 force field. Kollman charges and polar hydrogens were then added using AutoDock Tools. The docking grid was generated using the active site's residues listed in **Table 1**. The structures of the ligands, MeT (PubChem CID: 4091), furanone C-30 (PubChem CID: 10131246), 3-oxo-C12-HSL (PubChem CID: 3246941), C4-HSL (PubChem CID: 443433), and PQS (PubChem CID: 2763159), were obtained from PubChem in sdf format, converted to 3D structures with polar hydrogens using Open Babel, and molecular docking was conducted using AutoDock Vina (Version 1.5.4) with an exhaustiveness of '24.' The best binding pose was selected based on the predicted binding energy and molecular interactions. Docking conformations of each ligand were analyzed by examining their binding energy score (kcal/mol). The docking score of MeT was compared with the natural ligand of each QS receptor and furanone C-30, a known QS inhibitor.

3.8. RNA isolation and quantitative RT-PCR (qPCR)

Following treatment with MeT, the relative expression of QS- (*lasR*/*lasI*, *rhlR*/*rhlI*, and *pqsA*/*pqsR*) and virulence genes (*aprA*, *plcH*, *rhlAB*, and *toxA*) was assessed in *P. aeruginosa* PAO1 and PA14 [10]. Briefly, cell density was normalized (A_{600} ~ 0.8) and the cultures were harvested by centrifugation. Cell pellets were washed twice with DEPC-treated water. Total RNA was then isolated from treatment and control groups using Tri-Xtract™ reagent (G-Biosciences, MO, USA) according to the manufacturer's protocol. First-strand cDNA was synthesized using iScript Reverse Transcription kit (Bio-Rad, USA) and the gene expression was quantified using qPCR with previously defined primer pairs. The reactions were carried out using iQ™ SYBR® Green Supermix (Bio-Rad, CA, USA) with previously defined primer pairs [10], and glyceraldehyde-3-phosphate dehydrogenase (GAPDH) was used as an internal control to normalize gene expression. The experiment was performed in triplicates, and the relative gene expression was calculated using the $2^{-\Delta\Delta Ct}$ method [22].

3.9. Effect on QS-regulated virulence factors of P. aeruginosa

The phenotypic expression of hallmark QS-regulated pseudomonal virulence factors was examined following MeT treatment. Concisely, PAO1 and PA14 cultures were raised in the presence and absence of MeT, followed by normalization of cell density (A_{600} ~ 0.8). Cell-free supernatant was harvested by centrifugation and previously established procedures were employed to evaluate the production of alginate, cell-free hemolysin, pyochelin, pyocyanin, elastase and total protease activity [10,11]. The results were compared to the control (untreated) group and the percent inhibition or fold reduction was calculated.

3.10. Effect on motility phenotypes of P. aeruginosa

The anti-motility effects of MeT were investigated against *P. aeruginosa*. To examine twitching and swimming motility, the bacteriological media was surface inoculated with 2 µL of MeT-treated and -untreated bacterial cultures (A_{600} ~ 0.4), while swarming motility plates were inoculated by stabbing bacterial culture using sterile toothpicks. Post-24 h incubation, the motility phenotypes were assessed by measuring the diameters of bacterial growth or circular expansion around the point of inoculation, as described elsewhere [10,11].

Preprints (www.preprints.org) | NOT PEER-REVIEWED | Posted: 25 April 2023 doi:10.20944/preprints202304.0914.v1

3.11. Examining the anti-fouling prospects of MeT

3.11.1. Quantitative biofilm inhibition assay

The effectiveness of MeT in preventing pseudomonal biofilm formation was evaluated through a quantitative crystal violet (CV)-binding assay [10]. MeT was added to LB-containing wells, which were then inoculated with PAO1/PA14 cultures (1×10^6 CFU/mL) and incubated at 37ºC under static conditions. After 24 hours, the spent media was removed, and the wells were washed with PBS (pH 7.2) three times. The biofilms were then stained using 0.1% CV for 15 min at room temperature. Wells were washed with PBS again to remove excess dye, and the plate was air-dried at 37 ºC. The bound dye was eluted in 33% glacial acetic acid, and A_{595} values were measured using an ELISA plate reader (Bio-Rad, Hercules, CA). All experimental sets were processed similarly each day and biofilm formation was monitored for 9 days.

3.11.2. Extraction & estimation of total biofilm protein

Total biofilm protein was quantified as a function of pseudomonal biofilm population density on the test tube surface [34]. *P. aeruginosa* cultures were grown in LB tubes containing MeT for 4 days. The spent medium was replaced with fresh LB and MeT after every 24 hours. After 4 days of continuous growth, the spent medium was removed; the tubes were gently washed with PBS, and subsequently boiled for 30 minutes in the presence of 5 N NaOH (4 mL). The suspension was then vortexed and centrifuged at 8,000 x *g* for 15 minutes. Braford's assay was used to estimate the total protein content (in µg/mL) in the supernatant by normalizing the A_{595} values to a standard curve of bovine serum albumin.

3.11.3. Extraction & estimation of total biofilm exopolysaccharides (EPS)

Total exopolysaccharides in *P. aeruginosa* biofilms were quantified as a function of biofilm production. Briefly, *P. aeruginosa* biofilms were raised for 4 days, as described in the previous section [35]. The biofilms was then extracted in sterile distilled water and the resulting suspension was centrifuged. The supernatant was discarded, and the cell pellet was resuspended in a high salt buffer (10 mM KPO_4, 5 mM NaCl, 25 mM $MgSO_4$) by vortexing for 15 minutes to extract the cell-bound EPS. The suspension was then centrifuged, and the resulting supernatant was mixed with three volumes of chilled absolute ethanol (EtOH) and incubated at -20ºC for 4 hours. The solution was centrifuged again, and the pellet containing EPS was resuspended in sterile water. The concentration of EPS (in µg/mL) was estimated using a previously described phenol-sulfuric acid-based colorimetric assay [1]. The data was then normalized to a carbohydrate standard curve (fructose-sucrose).

3.11.4. Isolation and qualitative estimation of extracellular DNA (eDNA) from P. aeruginosa biofilms

To evaluate the impact of MeT on pseudomonal biofilms, extracellular DNA (eDNA) profiles were qualitatively examined. Concisely, eDNA was isolated from MeT-treated and -untreated biofilms with minor modifications [36]. The bacterial culture was centrifuged at 8,000 x *g* for 15 min at 4ºC and eDNA was precipitated by adding ice-cold 70% EtOH and 0.3 M sodium acetate (pH 8.0). The pellet-containing eDNA was air-dried and then dissolved in TE buffer (pH 8.0). The eDNA samples (5 µL) were then electrophoresed alongside a 1 kb DNA ladder in a 0.8% agarose gel, and changes in the eDNA profile were visualized under a UV transilluminator.

3.11.5. Microscopic evaluation of P. aeruginosa biofilms

To visualize pseudomonal biofilms following MeT treatment, field emission scanning electron microscopy (FESEM) was performed [10]. Biofilms were raised for 4 days on sterile coverslips in LB medium containing MeT. Fresh LB supplemented with MeT was replenished after every 24 h. Post-incubation, mature biofilms were fixed with 2% glutaraldehyde for 2 h and subsequently washed with PBS. The biofilms were then dehydrated using a gradient of EtOH (30%, 50%, 70%, 90%, and

100%), followed by air-drying, gold-coating, and visualization under FESEM (SU8010, Hitachi, Tokyo, Japan) at the Sophisticated Analytical Instrumentation Facility (SAIF), Panjab University, Chandigarh.

3.12. Statistical analysis

All experiments were performed using three biological triplicates, and the mean values along with standard deviations were determined. Each experiment was performed thrice, independently. The significance of data was assessed using GraphPad Prism (ver. 8.0) with one-way analysis of variance (ANOVA) test, and multiple comparisons (between groups) were examined using Tukey's multiple comparisons test. A p-value of less than 0.05 was deemed statistically significant (*p*-values: * ≤ 0.05, ** ≤ 0.01, *** ≤ 0.001, **** ≤ 0.0001).

4. Conclusion

Based on the comprehensive experimentation undertaken in this study, MeT was shown to harbor QQ properties. The results confirmed that sub-lethal concentrations of MeT disrupt the QS circuitry of *P. aeruginosa* by abrogating AHL biosynthesis. Additionally, MeT could effectively downregulate the expression of QS genes (*pqsA*/*pqsR*, *rhlI*/*rhlR*, and *lasI*/*lasR*) and QS-modulated virulence genes (*lasA*, *lasB*, *toxA*, *aprA*, & *plcH*) in *P. aeruginosa*, thereby inhibiting the production of hallmark virulence factors at phenotypic level and attenuating bacterial virulence. MeT was also predicted to strongly associate with the QS receptors of *P. aeruginosa*, which may be responsible for augmenting its anti-virulence potential *in vitro*. This study also illustrates the anti-motility and anti-fouling potential of MeT against *P. aeruginosa*. Therefore, MeT proves to be a potent anti-virulence drug which can be repurposed against pseudomonal infections in clinical settings. Nonetheless, *in vivo* investigations are warranted to establish its efficacy for widespread application as an alternate medicine against *P. aeruginosa* infections.

Supplementary Materials: Figure S1. Resazurin dye reduction assay for determining the MICs of MeT against *P. aeruginosa* (A) PAO1 and (B) PA14; **Figure S2.** Molecular docking analysis predicting the probable interactions between Furanone C-30 (control) and various QS receptors of *P. aeruginosa* using AutoDock Vina (Version 1.2.0); **Figure S3.** Heat maps depicting the production of virulence factors in laboratory-maintained strains of *P. aeruginosa* following treatment MeT at sub-MICs.

Author Contributions: Conceptualization, J.C., K.H.; methodology, J.C, L.K., K.H.; software, J.C, L.K., P.G..; validation, J.C. and P.G..; formal analysis, S.C.; investigation, J.C., L.K., P.G.; resources, K.H. and S.C.; data curation, J.C. and K.H.; writing—original draft preparation, J.C.; writing—review and editing, J.C. and K.H.; supervision, K.H. All authors have read and agreed to the published version of the manuscript.

Funding: This research received no external funding.

Institutional Review Board Statement: Not applicable.

Informed Consent Statement: Not applicable.

Data Availability Statement: Data used to support the findings of this study are available from the corresponding author upon request.

Acknowledgments: Financial assistance from the Indian Council of Medical Research (ICMR), New Delhi for providing fellowship (JRF & SRF) to JC is humbly appreciated.

Conflicts of Interest: The authors declare no conflict of interest.

References

1. Chadha, J. In vitro effects of sub-inhibitory concentrations of amoxicillin on physiological responses and virulence determinants in a commensal strain of Escherichia coli. *Journal of Applied Microbiology* **2021**, *131*, 682-694, doi:10.1111/jam.14987.
2. Chadha, J.; Khullar, L. Subinhibitory concentrations of nalidixic acid alter bacterial physiology and induce anthropogenic resistance in a commensal strain of Escherichia coli in vitro. *Letters in Applied Microbiology* **2021**, *73*, 623-633, doi:10.1111/lam.13550.

3. Chadha, J.; Gupta, M.; Nagpal, N.; Sharma, M.; Adarsh, T.; Joshi, V.; Tiku, V.; Mittal, T.; Nain, V.K.; Singh, A.; et al. Antibacterial potential of indigenous plant extracts against multidrug-resistant bacterial strains isolated from New Delhi region. *GSC Biological and Pharmaceutical Sciences* **2021**, *14*, 185-196, doi:10.30574/gscbps.2021.14.2.0053.
4. Maeda, T.; García-Contreras, R.; Pu, M.; Sheng, L.; Garcia, L.R.; Tomás, M.; Wood, T.K. Quorum quenching quandary: resistance to antivirulence compounds. *The ISME Journal* **2011**, *6*, 493-501, doi:10.1038/ismej.2011.122.
5. Chadha, J.; Harjai, K.; Chhibber, S. Repurposing phytochemicals as anti-virulent agents to attenuate quorum sensing-regulated virulence factors and biofilm formation in Pseudomonas aeruginosa. *Microbial Biotechnology* **2021**, *15*, 1695-1718, doi:10.1111/1751-7915.13981.
6. Chadha, J.; Harjai, K.; Chhibber, S. Revisiting the virulence hallmarks of Pseudomonas aeruginosa: a chronicle through the perspective of quorum sensing. *Environmental Microbiology* **2021**, *24*, 2630-2656, doi:10.1111/1462-2920.15784.
7. Organization, W.H. WHO publishes list of bacteria for which new antibiotics are urgently needed. Available online: https://www.who.int/news/item/27-02-2017-who-publishes-list-of-bacteria-for-which-new-antibiotics-are-urgently-needed (accessed on 20th April).
8. Chadha, J.; Thakur, N.; Chhibber, S.; Harjai, K. A comprehensive status update on modification of foley catheter to combat catheter-associated urinary tract infections and microbial biofilms. *Critical Reviews in Microbiology* **2023**, 1-28, doi:10.1080/1040841x.2023.2167593.
9. Lee, J.; Zhang, L. The hierarchy quorum sensing network in Pseudomonas aeruginosa. *Protein & Cell* **2014**, *6*, 26-41, doi:10.1007/s13238-014-0100-x.
10. Chadha, J.; Ravi; Singh, J.; Harjai, K. α-Terpineol synergizes with gentamicin to rescue Caenorhabditis elegans from Pseudomonas aeruginosa infection by attenuating quorum sensing-regulated virulence. *Life Sciences* **2023**, *313*, 121267, doi:10.1016/j.lfs.2022.121267.
11. Chadha, J.; Ravi; Singh, J.; Chhibber, S.; Harjai, K. Gentamicin Augments the Quorum Quenching Potential of Cinnamaldehyde In Vitro and Protects Caenorhabditis elegans From Pseudomonas aeruginosa Infection. *Frontiers in Cellular and Infection Microbiology* **2022**, *12*, doi:10.3389/fcimb.2022.899566.
12. Lv, Z.; Guo, Y. Metformin and Its Benefits for Various Diseases. *Frontiers in Endocrinology* **2020**, *11*, doi:10.3389/fendo.2020.00191.
13. Wang, Y.-W.; He, S.-J.; Feng, X.; Cheng, J.; Luo, Y.-T.; Tian, L.; Huang, Q. Metformin: a review of its potential indications. *Drug Design, Development and Therapy* **2017**, *11*, 2421-2429, doi:10.2147/dddt.s141675.
14. Zhao, Y.; Chen, Z.; Chen, Y.; Xu, J.; Li, J.; Jiang, X. Synergy of Non-antibiotic Drugs and Pyrimidinethiol on Gold Nanoparticles against Superbugs. *Journal of the American Chemical Society* **2013**, *135*, 12940-12943, doi:10.1021/ja4058635.
15. Masadeh, M.M.; Alzoubi, K.H.; Masadeh, M.M.; Aburashed, Z.O. Metformin as a Potential Adjuvant Antimicrobial Agent Against Multidrug Resistant Bacteria. *Clinical Pharmacology: Advances and Applications* **2021**, *13*, 83-90, doi:10.2147/cpaa.s297903.
16. Nievas, F.; Bogino, P.; Sorroche, F.; Giordano, W. Detection, Characterization, and Biological Effect of Quorum-Sensing Signaling Molecules in Peanut-Nodulating Bradyrhizobia. *Sensors* **2012**, *12*, 2851-2873, doi:10.3390/s120302851.
17. Gui, M.; Liu, L.; Wu, R.; Hu, J.; Wang, S.; Li, P. Detection of New Quorum Sensing N-Acyl Homoserine Lactones From Aeromonas veronii. *Frontiers in Microbiology* **2018**, *9*, doi:10.3389/fmicb.2018.01712.
18. Harjai, K.; Gupta, P.; Chhibber, S. Subinhibitory concentration of ciprofloxacin targets quorum sensing system of Pseudomonas aeruginosa causing inhibition of biofilm formation & reduction of virulence. *Indian Journal of Medical Research* **2016**, *143*, 643, doi:10.4103/0971-5916.187114.
19. Yang, D.; Hao, S.; Zhao, L.; Shi, F.; Ye, G.; Zou, Y.; Song, X.; Li, L.; Yin, Z.; He, X.; et al. Paeonol Attenuates Quorum-Sensing Regulated Virulence and Biofilm Formation in Pseudomonas aeruginosa. *Frontiers in Microbiology* **2021**, *12*, doi:10.3389/fmicb.2021.692474.
20. Kumar, L.; Brenner, N.; Brice, J.; Klein-Seetharaman, J.; Sarkar, S.K. Cephalosporins Interfere With Quorum Sensing and Improve the Ability of Caenorhabditis elegans to Survive Pseudomonas aeruginosa Infection. *Frontiers in Microbiology* **2021**, *12*, doi:10.3389/fmicb.2021.598498.
21. Kumar, L.; Chhibber, S.; Kumar, R.; Kumar, M.; Harjai, K. Zingerone silences quorum sensing and attenuates virulence of Pseudomonas aeruginosa. *Fitoterapia* **2015**, *102*, 84-95, doi:10.1016/j.fitote.2015.02.002.

22. Livak, K.J.; Schmittgen, T.D. Analysis of Relative Gene Expression Data Using Real-Time Quantitative PCR and the 2−ΔΔCT Method. *Methods* **2001**, *25*, 402-408, doi:10.1006/meth.2001.1262.
23. El-Mowafy, S.A.; Shaaban, M.I.; Abd El Galil, K.H. Sodium ascorbate as a quorum sensing inhibitor of Pseudomonas aeruginosa. *Journal of Applied Microbiology* **2014**, *117*, 1388-1399, doi:10.1111/jam.12631.
24. Dai, L.; Wu, T.-q.; Xiong, Y.-s.; Ni, H.-b.; Ding, Y.; Zhang, W.-c.; Chu, S.-p.; Ju, S.-q.; Yu, J. Ibuprofen-mediated potential inhibition of biofilm development and quorum sensing in Pseudomonas aeruginosa. *Life Sciences* **2019**, *237*, 116947, doi:10.1016/j.lfs.2019.116947.
25. Bajire, S.K.; Jain, S.; Johnson, R.P.; Shastry, R.P. 6-Methylcoumarin attenuates quorum sensing and biofilm formation in Pseudomonas aeruginosa PAO1 and its applications on solid surface coatings with polyurethane. *Applied Microbiology and Biotechnology* **2021**, *105*, 8647-8661, doi:10.1007/s00253-021-11637-9.
26. Seleem, N.M.; Atallah, H.; Abd El Latif, H.K.; Shaldam, M.A.; El-Ganiny, A.M. Could the analgesic drugs, paracetamol and indomethacin, function as quorum sensing inhibitors? *Microbial Pathogenesis* **2021**, *158*, 105097, doi:10.1016/j.micpath.2021.105097.
27. Shastry, R.P.; Ghate, S.D.; Sukesh Kumar, B.; Srinath, B.S.; Kumar, V. Vanillin derivative inhibits quorum sensing and biofilm formation in Pseudomonas aeruginosa: a study in a Caenorhabditis elegans infection model. *Natural Product Research* **2021**, *36*, 1610-1615, doi:10.1080/14786419.2021.1887866.
28. Kim, B.; Park, J.-S.; Choi, H.-Y.; Yoon, S.S.; Kim, W.-G. Terrein is an inhibitor of quorum sensing and c-di-GMP in Pseudomonas aeruginosa: a connection between quorum sensing and c-di-GMP. *Scientific Reports* **2018**, *8*, doi:10.1038/s41598-018-26974-5.
29. Murray, T.S.; Ledizet, M.; Kazmierczak, B.I. Swarming motility, secretion of type 3 effectors and biofilm formation phenotypes exhibited within a large cohort of Pseudomonas aeruginosa clinical isolates. *Journal of Medical Microbiology* **2010**, *59*, 511-520, doi:10.1099/jmm.0.017715-0.
30. Daniels, R.; Vanderleyden, J.; Michiels, J. Quorum sensing and swarming migration in bacteria. *FEMS Microbiology Reviews* **2004**, *28*, 261-289, doi:10.1016/j.femsre.2003.09.004.
31. Williams, P.; Cámara, M. Quorum sensing and environmental adaptation in Pseudomonas aeruginosa: a tale of regulatory networks and multifunctional signal molecules. *Current Opinion in Microbiology* **2009**, *12*, 182-191, doi:10.1016/j.mib.2009.01.005.
32. Moradali, M.F.; Ghods, S.; Rehm, B.H.A. Pseudomonas aeruginosa Lifestyle: A Paradigm for Adaptation, Survival, and Persistence. *Frontiers in Cellular and Infection Microbiology* **2017**, *7*, doi:10.3389/fcimb.2017.00039.
33. Wiegand, I.; Hilpert, K.; Hancock, R.E.W. Agar and broth dilution methods to determine the minimal inhibitory concentration (MIC) of antimicrobial substances. *Nature Protocols* **2008**, *3*, 163-175, doi:10.1038/nprot.2007.521.
34. Das, M.C.; Sandhu, P.; Gupta, P.; Rudrapaul, P.; De, U.C.; Tribedi, P.; Akhter, Y.; Bhattacharjee, S. Attenuation of Pseudomonas aeruginosa biofilm formation by Vitexin: A combinatorial study with azithromycin and gentamicin. *Scientific Reports* **2016**, *6*, doi:10.1038/srep23347.
35. Bose, S.K.; Nirbhavane, P.; Batra, M.; Chhibber, S.; Harjai, K. Nanolipoidal α-terpineol modulates quorum sensing regulated virulence and biofilm formation in Pseudomonas aeruginosa. *Nanomedicine* **2020**, *15*, 1743-1760, doi:10.2217/nnm-2020-0134.
36. Moshynets, O.V.; Baranovskyi, T.P.; Iungin, O.S.; Kysil, N.P.; Metelytsia, L.O.; Pokholenko, I.; Potochilova, V.V.; Potters, G.; Rudnieva, K.L.; Rymar, S.Y.; et al. eDNA Inactivation and Biofilm Inhibition by the PolymericBiocide Polyhexamethylene Guanidine Hydrochloride (PHMG-Cl). *International Journal of Molecular Sciences* **2022**, *23*, 731, doi:10.3390/ijms23020731.